Journal of Transactions in Systems Engineering
https://journals.tultech.eu/index.php/jtse
ISSN: 2806-2973
Volume 2, Issue 3
DOI: https://doi.org/10.15157/jtse.2024.2.3.282-294
Received: 16.08.2024; Revised: 26.09.2024; Accepted: 04.10.2024

Research Article

Effect of Heat Treatment on Mechanical Properties and Corrosion Resistance of β Ti-18Mo-xCr (x = 3 & 7 wt.%) Alloy

Rosita Utari[1], Bunga Rani Elvira[2], Ika Kartika[2], Alfirano[1] and Galih Senopati[2]*

[1]Metallurgical Engineering Department, University of Sultan Ageng Tirtayasa, Banten, 42435, Indonesia

[2] Research Centre for Metallurgy, National Research and Innovation Agency (BRIN), KST BJ Habibie, South Tangerang, Banten, 15314, Indonesia

*** galih.senopati@brin.go.id**

Abstract

β-Titanium alloys have gained significant attention for orthopaedic implants due to their superior mechanical properties, including high strength and a notably lower elastic modulus compared to conventional Ti-6Al-4V alloys. In this study, Ti-18Mo-xCr (x = 3 and 7 wt.%) alloys were developed to explore novel materials for biomedical applications. The alloys were produced using Vacuum Arc Remelting (VAR) followed by solution treatment and aging heat treatments. The elastic modulus was assessed using the Sonelastic tool, while corrosion resistance was evaluated via electrochemical polarization in a 0.9% NaCl solution. Surface morphology post-corrosion was analysed using SEM-EDS. The solution-treated alloys exhibited a significantly lower elastic modulus than those subjected to aging. Furthermore, the corrosion resistance of the aging-treated alloys was markedly inferior to both the solution-treated samples and the Ti-6Al-4V alloy, primarily due to β-phase stabilization during solution treatment. Prolonged aging further compromised corrosion resistance. Among all tested conditions, the Ti-18Mo-3Cr alloy aged at 500 °C demonstrated the lowest corrosion rate of 7.7373×10^{-5} mm/year. These findings highlight the potential of Ti-18Mo-xCr alloys as candidates for next-generation orthopaedic implants, balancing mechanical properties and corrosion resistance.

Keywords: β-titanium, elastic modulus, corrosion resistance, solution treatment, aging

INTRODUCTION

One major cause of bone fractures is road traffic accidents, which represent a significant public health issue. The World Health Organization reports a concerning rise in fatalities and injuries due to traffic accidents worldwide. This growing trend underscores the urgent need for improved safety measures, preventive strategies, and advanced medical interventions to mitigate the impact of traffic-related injuries, including the development of innovative treatments for bone fractures [1-8]. Traffic accidents were predicted to be the third most common cause of injury and death globally in 2020. Statistics from Indonesia's Central Statistics Agency support this trend, showing an average yearly rise in road accidents of 0.77% from 2013 to 2017. The aforementioned figures underscore the consistent

upward trend in traffic incidents and underscore the imperative requirement for improved road safety protocols and regulatory measures to mitigate the societal and healthcare costs linked to injuries sustained in traffic [1, 9-12]. Bone fractures often require the use of implants to facilitate the healing process. When implanted in the human body, these devices are exposed to various corrosive environments, such as bodily fluids, which can trigger corrosion reactions. Therefore, it is essential that the materials used in implants possess the characteristics of biomaterials. A fundamental requirement of biomaterials is biocompatibility—the ability of the implant to integrate with body tissues and fluids without eliciting adverse reactions. Ensuring biocompatibility is crucial for the success of implants in promoting safe and effective healing [2, 13-17]. This emphasizes how crucial it is to consider the psychological state of the body, which is best described as a condition of inertia—a resistance to deterioration. When an implant is used in terms of this, it should have the capacity to withstand biological and chemical reactions inside the body—while maintaining long-term stability and functionality in vivo [3, 18-21].

Corrosion of biomaterials is an important aspect of biocompatibility, and only the noble metals (such as the gold and platinum group metals) or the most passive metals (such as titanium or chromium) have corrosion rates at apparently acceptable levels [2]. Corrosion of implants in body fluid media occurs through electrochemical reactions [4]. Additionally, it is necessary to know the electrochemical principles most relevant to the corrosion process. The alloy metal components are oxidized to their ionic form (anode), and dissolved oxygen is reduced to hydroxyl ions (cathode) [5].

Biomaterials used as bone implants will be continuously designed to be accepted by the body and not cause reactions to body fluids in the long or short term. The most widely selected titanium alloy as an implant material is the Ti-6Al-4V alloy, which has an α+β phase [6]. The material to be used as an implant must have a low elastic modulus or be close to the bone, especially the cortical bone, which is 10–30 GPa. Meanwhile, the elastic modulus value in the Ti-6Al-4V alloy is still very high at 110 GPa [7]. Lower elastic modulus than the bone can experience stress shielding [22-27].

One of the methods to reduce elastic modulus in titanium alloys is through a heat treatment process to obtain the β phase [28]. The β phase is targeted because it can reduce the value of the elastic modulus. In a study conducted by Elshalakany et al. in 2017, using the Ti-18Mo-xCr alloy in the solution treatment process reduced the elastic modulus up to 86 GPa [10]. In another study conducted by Winda in 2019 regarding the effect of aging time on the mechanical properties of titanium alloys, it was found that samples with the aging treatment with the longest holding time of 8 hours had the highest elongation of 4.5% and the highest strength of 881 MPa [11]. This shows that high strength is expected to reduce the value of the elastic modulus.

In addition to affecting the decrease in the elastic modulus value, the β phase can also increase the corrosion resistance of a material. In a study conducted by Nishimura et al. (2010), the results of tests using the polarization method on titanium alloys showed that the corrosion resistance of samples subjected to aging treatment, which produced α-phase, showed lower corrosion resistance than samples subjected to solution treatment, which

produced β-phase [12]. Then, in another study conducted by Winda in 2019 concerning the effect of aging time on the corrosion resistance of titanium alloys, it was found that samples with aging treatment with the longest holding time of 8 hours had the lowest corrosion rate of 0.81 mpy [11]. Therefore, this research was conducted to find the composition of the Ti-18Mo-xCr (3 and 7% wt) alloy, which has a low elastic modulus and high corrosion resistance, as an alternative to the commercial titanium alloy Ti-6Al-4V for orthopedic implant applications.

MATERIALS AND METHODS

Ti-18Mo-xCr alloy with Cr composition variations of 3 and 7 wt.% sample preparation was carried out as cast using VAR with an argon vacuum. The chemical compositions of the alloys are shown in Table 1.

Table 1. Element composition of the experimental alloys (wt.%).

Alloy	Cr	Mo	Ti	Unit
3Cr	2,73	17,17	Bal.	w.t.%
7Cr	7,13	17,78	Bal.	w.t.%

The Ti-18Mo-xCr alloy was cast using a specialized technique called vacuum Arc Remelting (VAR), employing ultra-high purity argon gas in the process [14]. Then, the chemical composition analysis was carried out using the Optical Emission Spectroscopy (OES) Bruker Q4 Tasman equipment. After the casting process, the as-cast sample underwent a Solution Treatment at a temperature of 850 °C for 1 hour using a tube furnace within an inert atmosphere of argon gas (called ST850). The sample was then rapidly quenched by placing it in water. The solution-treated sample was then subjected to an aging process at a temperature of 500 °C for a duration of 8 hours (called AT500) [12].
Metallographic observations were carried out to determine the phase characteristics and the precipitate formed in the Ti-18Mo-xCr sample and compare it to the Ti-6Al-4V sample regarding its corrosion resistance. The magnifications used for metallographic observations are 100X, 200X, 500X, and 1000X using an OLYMPUS Optical Microscope. The metallographic steps carried out in this research are framing the sample (mounting) using a clear resin, sanding the sample using a grinding machine with sandpaper sizes #80, #120, #400, #600, #800, #1000 to #1200, polishing using a colloidal silica solution, and etching using a mixed solution of 15% nitric acid and 5% hydrogen fluoride.

An X-ray diffraction (XRD) analysis was performed using the XRD Panalytical TD-3500 instrument to identify the phases formed at each stage of the process. The XRD in the PTBIN-BATAN Serpong lab used a Cu source with λ = 1,5406 Å and a measurement area of 2θ: 30°–80° with another component in the form of a cooler, which is used to cool because, during the X-ray formation process, the X-rays are emitted high energy and heat generation. The X-rays fired at the sample are high-powered electromagnetic waves ranging from about 200 eV to 1 MeV, located between ultra-violet and γ-rays. Then a set of computers and CPUs After getting data from each sample, the samples were analyzed using angles of 20◦ and 80◦ using HighScore Plus software. The 2θ angle is predicted to be

able to show the highest β-phase peak based on previous research at 200 peaks. Then the graph is made using Origin.

The modulus elasticity testing for each sample was carried out using a sonelastic tool. Sonelastic is a tool used to detect the value of the modulus elasticity of a material using a sensor to detect the response of the sample sound wave. This tool can detect samples with an elastic modulus ranging from 0.5 to 1000 GPa and dimensions between 1 cm and 5.3 m [10]. This test was carried out using the ASTM E-1876-01 [15] standard. The hardness testing was performed using the Mitutoyo Vickers microhardness tester, applying a load of 1 N and allowing a dwell time of 12 seconds.

The electrochemical performance of the Ti-18Mo-7Cr alloy was assessed using the polarization method in a 0.9 NaCl solution. The tests were conducted in a three-electrode corrosion cell, with the Ti alloy serving as the working electrode, platinum wire as the counter electrode, and an Ag/AgCl electrode (saturated in KCl solution) as the reference electrode.

EXPERIMENTAL RESULTS

Figure 1 shows the results of the optical microscope observation of the as-cast Ti-18Mo-xCr (3 and 7 wt.%) alloy. It can be observed that the microstructure of the Ti-18Mo-xCr alloy has a fully acicular microstructure and has clear grain boundaries (βGB). The formation of βGB starts with the heating process of the titanium alloy. Several changes will occur, such as the transformation of the $\alpha \rightarrow \beta$ phase in small amounts, the low stress value, and the high diffusion coefficient of the bcc-β phase. The heating transformation process lasts only a short time, 50 seconds. The formation of βGB will initiate the formation of a continuous β phase using a phase shift [16]. This fully-acicular structure consists of brightly colored α-acicular nestled in a dark-colored β-retained matrix. While the prior phase is also called the matrix, which has a smaller and minority fraction than the acicular. The observations after heat treatment showed that the optical microscope resulted in a structure forming flat colonies containing several parallel and intersecting martensite-β blades with fairly wide grain boundaries [18].

While the morphology of the microstructure should be formed in the aging process of the lamellar phase, which is formed from the phase when cooling, However, due to the influence of the addition of alloying element stabilizers, namely Mo and Cr, the resulting structure becomes a flat colony as in the solution treatment process. Figure 1 shows the beta-dendritic structure with grain boundaries. The XRD data also shows that there is no precipitate phase other than the beta matrix.

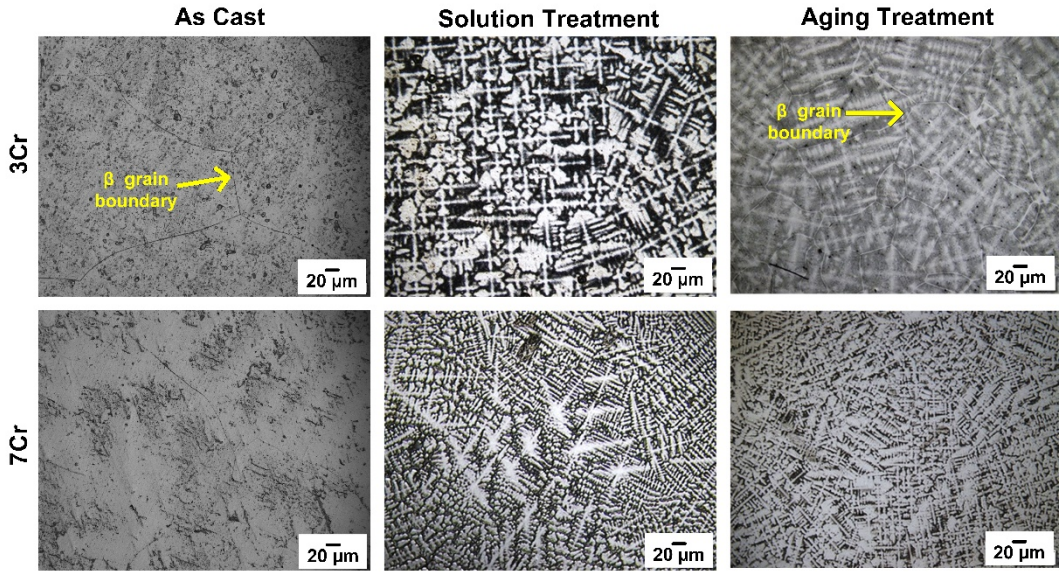

Figure 1. Microstructure of Ti-18Mo-xCr.

Figure 2 shows that pure titanium at room temperature will form an HCP crystal structure called the Alpha phase (α). This HCP structure is stable up to a temperature of 882°C. Meanwhile, above the temperature of 882 °C, the crystal structure will change to BCC, or what is called the beta (β) phase [18]. When pure titanium has a high heating temperature to reach the β phase, the addition of β phase stabilizers can reduce the β transus temperature. This β-phase stabilizer is divided into β-eutectoid and β-isomorphous. The difference lies in the dissolution process; β-isomorphous stabilizers can dissolve completely in β titanium alloys such as Nb, Mo, and V. Meanwhile, β-eutectoid stabilizers have limited solubility. Alloys with β phase stabilizing elements, when cooled rapidly (quenching), can form α martensite structures in β phase [19].

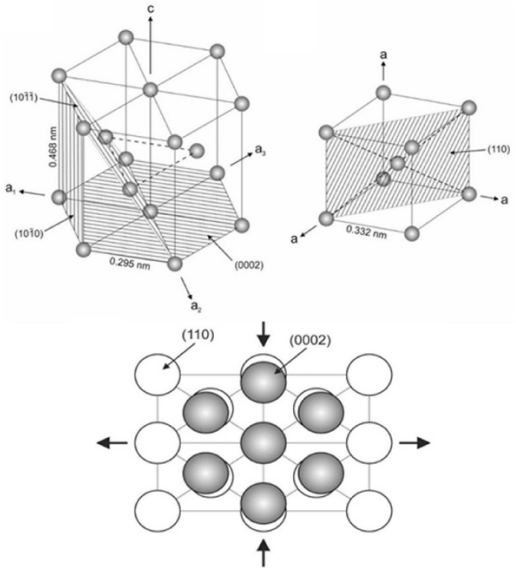

Figure 2. Titanium Crystal Structure [20].

The XRD results, presented in Figure 3, not only confirm the presence of β-phase XRD peaks but also indicate the lattice parameters consistent with a unit cell where a = b = c, characteristic of a Body Center Cubic (BCC) crystal structure. The intensity of the β-phase peaks reflects a composition that is entirely composed of 100% β-phase. Notably, the XRD characterization shown in Figure 2 reveals no peaks corresponding to the α phase, even after aging treatment. This absence can be attributed to the β-phase stabilizing elements incorporated into this alloy. As a result, the formation of new α-phase precipitates from the β matrix is effectively suppressed, leading to a stable β-phase structure.

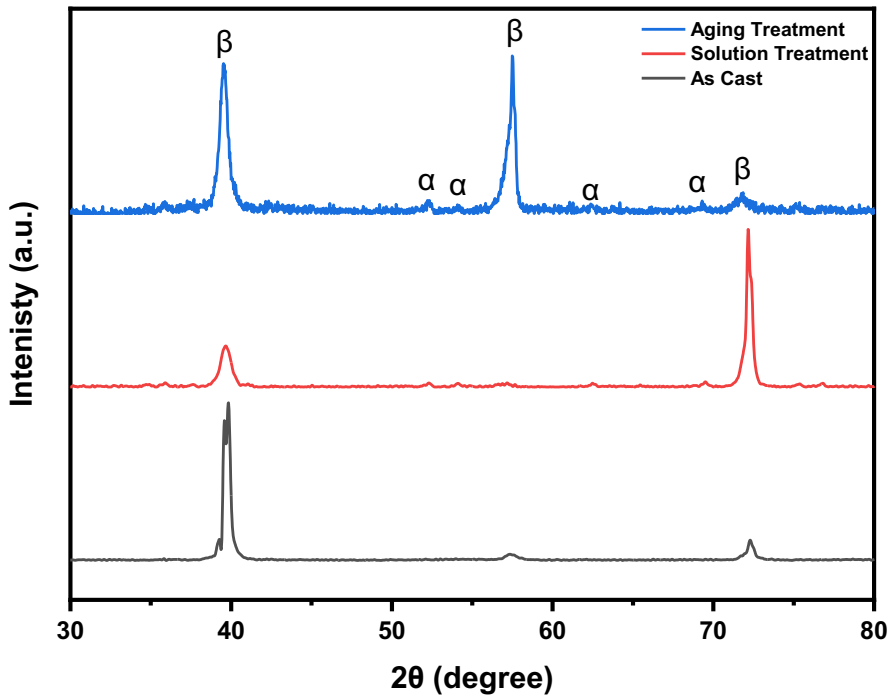

Figure 3. XRD Ti-18Mo-7Cr Alloy.

The XRD analysis reveals that, in the as-cast condition, the predominant phase in the alloy is β-phase, exhibiting the highest peak intensity among the samples studied. In contrast, alloys subjected to aging treatment with extended heating times show a notable reduction in peak height. This variation in peak height correlates with the microstructural morphology observed. Without heat treatment, the alloy develops a nearly uniform β-prior grain structure. However, prolonged heat treatment leads to forming a columnar β-prior grain structure [21].

The observed differences in peak height are significantly influenced by the concentration of chromium (Cr) alloying elements. A higher diffraction angle indicates decreased interplanar spacing within the alloy [22]. During the aging process, the growth of the α grain boundary (αGB) is notably affected by the presence of 7 wt% Cr. Increased Cr content enhances the diffusion coefficient, surpassing that of molybdenum (Mo), contributing to an accelerated growth rate of the αGB. This observation is further

supported by the XRD results, which indicate that the reduced interplanar distance within the β phase facilitates the β→α phase transformation during heat treatment [23].

One of the critical mechanical properties to consider for orthopedic implant materials is the elastic modulus, which is closely linked to material strength; specifically, a lower elastic modulus typically indicates greater strength [10]. As shown in Figure 4, the heat-treated alloy exhibits a lesser tendency to decrease its elastic modulus compared to the as-cast alloy. Although the XRD results for the as-cast alloy indicate the presence of the α-phase, it still displays a high elastic modulus due to the uneven distribution of the β-phase within the alloy.

This observation underscores the effectiveness of the phase stabilizing elements, namely molybdenum (Mo) and chromium (Cr), in reducing the elastic modulus compared to the α+β phase observed in the Ti-6Al-4V alloy. When examining the results of the solution-treated alloy in detail, it is evident that it tends to have a lower elastic modulus than its aged counterpart. This phenomenon occurs because the heating process applied to the sample below the transus temperature promotes the formation of phase precipitates, which can consequently elevate the elastic modulus.

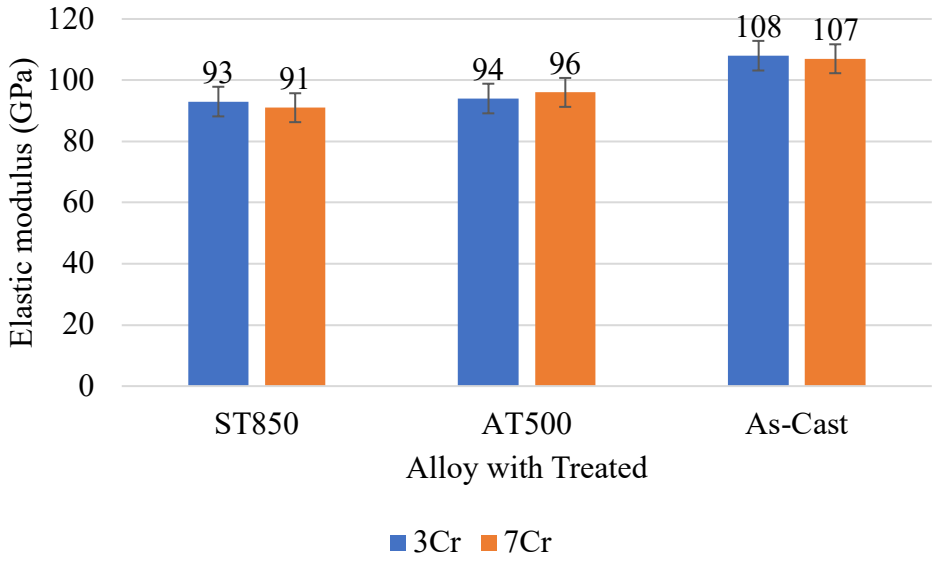

Figure 4. XRD Ti-18Mo-7Cr Alloy.

The results of hardness testing using Vickers microhardness can be seen in Figure 5. From the test results, it can be seen that the sample with solution treatment tends to have a higher hardness value compared to aging and as-cast alloys. The results of this test are inversely proportional to the results of the elastic modulus testing; namely, the lower the value of the elastic modulus of a material, the greater its hardness (strength). In addition, solution-treated alloys have higher hardness values due to rapid cooling so that the phase grains do not have much time to develop, and the addition of phase-stabilizing elements can maintain the β-phase strongly to produce higher hardness values. While aging with a long holding time is used to increase the material's ductility, this occurs due to the

metastable phase transformation that occurs after age-hardening treatment. The finer the deposit, the higher the hardness. If a material's strength (hardness) increases, it will decrease the ductility of the material. This is related to the diffusion mechanism, namely that the longer the aging time, the longer the unstable phase of the treatment solution will diffuse so that the phase becomes more stable [11].

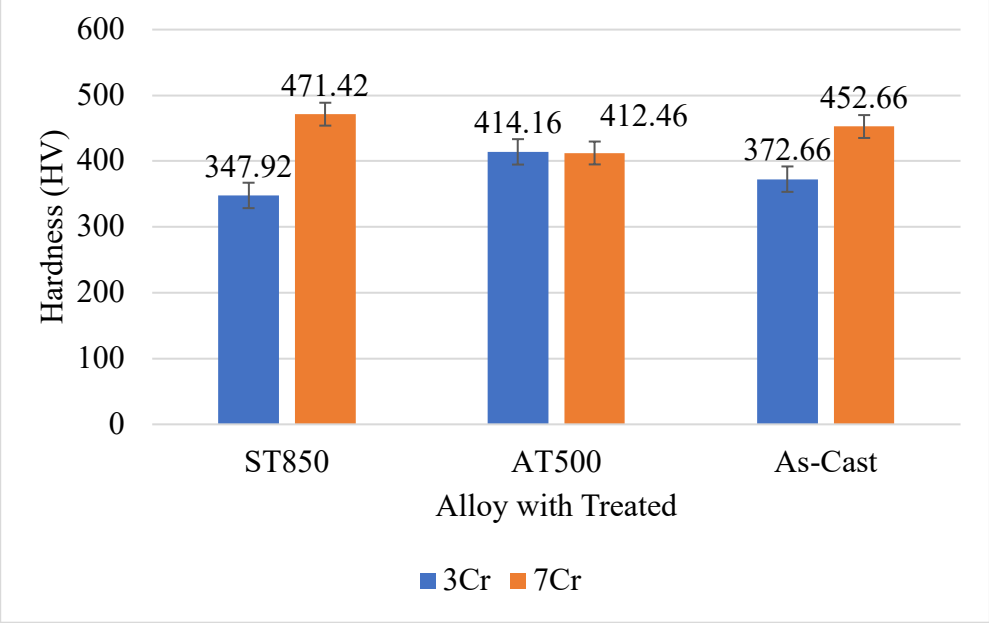

Figure 5. Graph of Ti-18Mo-xCr Alloys on Hardness.

Corrosion test results can be seen in Figure 6. Corrosion test results show that the corrosion rate value of the Ti-6Al-4V alloy used as a comparison has a corrosion rate value that is lower than the corrosion rate value allowed for implant applications based on European standards, which is 0.457 mpy [24]. The corrosion rate of the Ti-6Al-4V alloy is known to be 0.72094 mmpy. Meanwhile, the Ti-18Mo-7Cr ST850 alloy has a lower corrosion rate than the commercial titanium alloy Ti-6Al-4V, which is 0.009228 mmpy. The corrosion rate results in this aging alloy are much lower than those of the ST850 alloy and Ti-6Al-4V alloy. This is because the β phase can still be maintained even in the aging process. In addition to the β phase stabilizer, the heating temperature used is still in the metastable phase, which helps in increasing the corrosion resistance of the alloy [2]. Furthermore, the Ti-18Mo-3Cr AT500 alloy has the lowest corrosion rate among the samples in this study, which is 7.7373X10-5 mmpy.

Observations using optical microscopy before and after corrosion testing reveal significant changes in the surface characteristics of the alloys. In the Ti-18Mo-3Cr ST850 alloy, the post-corrosion test surface exhibited increased roughness and turbidity, with clear indications of pitting corrosion. The presence of oxidation was further evidenced by a purplish discoloration on the surface. In contrast, the Ti-18Mo-3Cr AT500 alloy maintained a surface appearance similar to that observed before testing, although optical microscopy revealed signs of pitting corrosion as well.

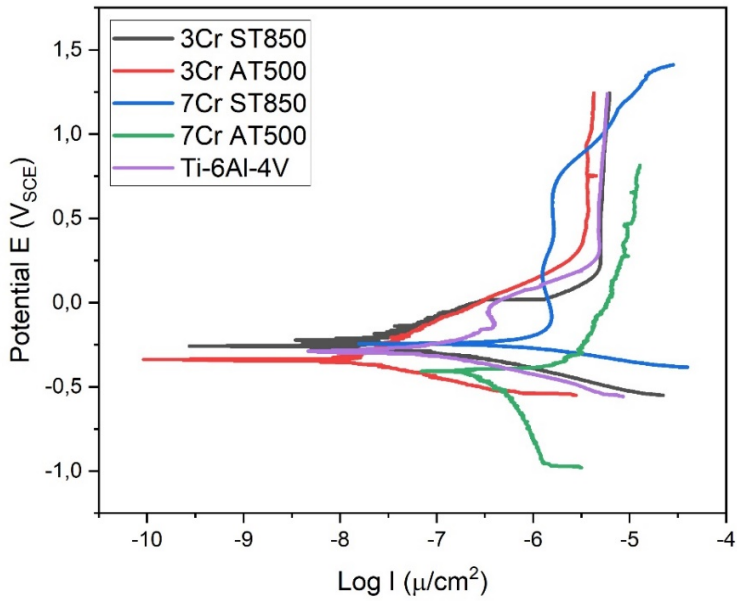

Figure 6. Tafel Polarization Ti-18Mo-xCr Alloy.

When compared to the Ti-6Al-4V alloy, the surface characteristics before and after corrosion testing showed minimal differences. However, upon microscopic examination, the surface displayed increased cloudiness and several small dark pits, indicating localized corrosion. These findings underscore the varying corrosion behaviors of the alloys, highlighting the effects of composition and processing on their surface integrity post-corrosion testing. Figure 7 shows the formation of a number of pores after the corrosion test. This was confirmed by SEM observations, which showed compatibility with the Ti-18Mo-xCr alloy in Figure 8.

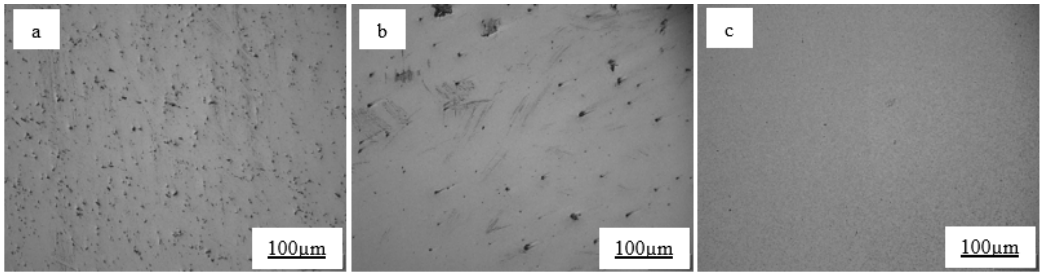

Figure 7. Ti-18Mo-3Cr Alloy Morphology SEM-EDS After Corrosion Testing.

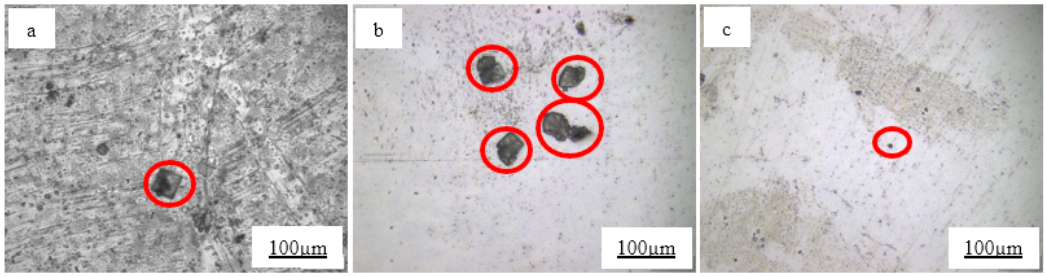

Figure 8. Ti-18Mo-3Cr Alloy Morphology After Corrosion Testing.

Microscopic observations are further corroborated by SEM-EDS analysis. In the Ti-18Mo-3Cr ST850 alloy, as illustrated in Figure 9, point 001 reveals a decrease in mass percentage of both chromium (Cr) and molybdenum (Mo) within the pitting corrosion potential area. In contrast, point 003 exhibits a homogeneous mass composition in the base metal. For the Ti-18Mo-3Cr AT500 alloy, point 002 in the pitting corrosion potential area indicates a decrease in mass percentage of molybdenum. This alloy demonstrates minimal pitting corrosion, as oxidation did not significantly alter the sample's color after corrosion testing. When compared to the commercial Ti-6Al-4V alloy, the Ti-18Mo-3Cr alloys exhibit less and smaller instances of pitting corrosion; however, signs of pitting remain evident at point 003, marked by a darker coloration. Notably, additional elements such as carbon (C), oxygen (O), and chlorine (Cl) are detected in substantial mass percentages. This phenomenon arises because the pitting-affected surface has reacted with the oxidized 0.9% NaCl solution, leading to the formation of Cl^- ions that contribute to the breakdown of the passive film under increased potential, resulting in observable pitting corrosion on the alloy surface [26].

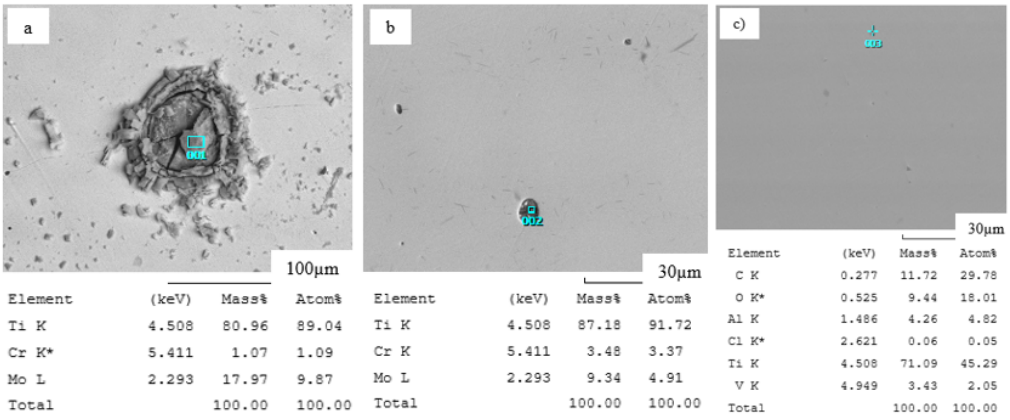

Element	(keV)	Mass%	Atom%
Ti K	4.508	80.96	89.04
Cr K*	5.411	1.07	1.09
Mo L	2.293	17.97	9.87
Total		100.00	100.00

Element	(keV)	Mass%	Atom%
Ti K	4.508	87.18	91.72
Cr K	5.411	3.48	3.37
Mo L	2.293	9.34	4.91
Total		100.00	100.00

Element	(keV)	Mass%	Atom%
C K	0.277	11.72	29.78
O K*	0.525	9.44	18.01
Al K	1.486	4.26	4.82
Cl K*	2.621	0.06	0.05
Ti K	4.508	71.09	45.29
V K	4.949	3.43	2.05
Total		100.00	100.00

Figure 9. Ti-18Mo-3Cr Alloy Morphology SEM-EDS After Corrosion Testing.

CONCLUSION

Based on the investigation of heat treatment effects, specifically solution treatment and aging treatment on the Ti-18Mo-xCr alloy (x = 3 and 7 wt%), the following conclusions can be drawn:

1. The microstructure observed in both solution-treated and aged samples is fully equiaxed, characterized by martensitic colonies in flat formations. This microstructure is influenced by the presence of retained phases, resulting from rapid cooling through water quenching during solution treatment. In the aging process, the β phase remains stable due to the elevated heating temperature, placing the material in a metastable β-phase region. In contrast, the Ti-6Al-4V alloy exhibits a characteristic α+β microstructure, typical of its composition.
2. A lower elastic modulus in a material correlates with higher hardness, attributable to the formation of a more stable phase. Consequently, the alloy in the solution-

treated state exhibits a lower elastic modulus compared to the aged alloy. Among the tested samples, Ti-18Mo-7Cr ST850 demonstrates the lowest elastic modulus of 91 GPa, coupled with the highest hardness value of 471.42 HV, highlighting its superior mechanical performance.

3. The corrosion rate significantly decreases with extended aging time, particularly after 8 hours, yielding a much lower corrosion rate compared to solution-treated samples. Among the tested alloys, Ti-18Mo-3Cr aged at 500°C (AT500) exhibits the lowest corrosion rate of 7.7373×10^{-5} mmpy, which is notably lower than the corrosion rate of the Ti-6Al-4V alloy, measured at 0.04389 mmpy. This demonstrates the superior corrosion resistance of the Ti-18Mo-3Cr AT500 alloy.

ACKNOWLEDGMENT

The authors acknowledge the Nanotechnology and Materials Research Organization BRIN for providing a portion of the funding for this study.

CONFLICT OF INTERESTS

The authors would like to confirm that there is no conflict of interests associated with this publication and there is no financial fund for this work that can affect the research outcomes.

REFERENCES

1. Amak, B., Malonda, N. S. H., & Kawatu, P. A. T. Hubungan Perilaku Safety Riding Pengendara Ojek Online Dengan Kejadian Kecelakaan Lalulintas Di Kota Manado Bryanza. *Jurnal of Public Health and Community Medicine* **2020**; 1(1); pp. 45–51.
2. Ige, O. O., Umoru, L. E., Adeoye, M. O., Adetunji, A. R., Olorunniwo, O. E., & Akomolafe, I. I. Monitoring, control and prevention practices of biomaterials corrosion - An overview. *Trends in Biomaterials and Artificial Organs* **2009**; 23(2); pp. 93–104.
3. Denstedt, J., & Atala, A. Biomaterials and Tissue Engineering in Urology. *Biomaterials and Tissue Engineering in Urology* **2009**; 28(August); 1–568.
4. McNeil, A. J. S. Corrosion: Vol. 1, metal/environment reactions; vol. 2, corrosion control. *Surface Technology* **1977**; 6(2); pp. 151–152.
5. Kamachi Mudali, U., Sridhar, T. M., & Baldev, R. A. J. Corrosion of bio implants. Sadhana - *Academy Proceedings in Engineering Sciences* **2003**; 28(3–4); pp. 601–637.
6. ASTM F136-08. Standard Specification for Wrought Titanium-6Aluminum-4Vanadium ELI (Extra Low Interstitial) Alloy for Surgical Implant Applications. *ASTM International*, 6–9.
7. Niinomi, M., Liu, Y., Nakai, M., Liu, H., & Li, H.. Biomedical titanium alloys with Young's moduli close to that of cortical bone. *Regenerative Biomaterials* **2016**; 3(3); pp. 173–185.
8. Purna Sari, B. (2017). Pengaruh Temperatur Pemanasan dan Laju Pendinginan Terhadap Struktur Mikro dan Modulus Elastisitas Paduan Ti-6Al-4V untuk Aplikasi Biomedis. Universitas Sultan Ageng Tirtayasa (Indonesian Language).

9. Alfirano, S.S. Friandani & C. Sutowo. Effect of solution treatment on the microstructure and mechanical properties of Ti-6Al-6Mo hot-rolled alloy, *Journal of Mechanical Engineering and Sciences*, **2019**; 13(2); pp. 4857-68.
10. Elshalakany, A. B., Ali, S., Amigó Mata, A., Eessaa, A. K., Mohan, P., Osman, T. A., & Amigó Borrás, V. Microstructure and Mechanical Properties of Ti-Mo-Zr-Cr Biomedical Alloys by Powder Metallurgy. *Journal of Materials Engineering and Performance* **2017**; 26(3); pp. 1262–1271.
11. Winda Magfira S. 2019. Studi Pengaruh Temperatur Solution Treatment dan Waktu Aging terhadap Sifat Mekanik Serta Ketahanan Korosi pada Paduan Implan Biomedis Ti-6Al-7Nb Hasil Centrifugal Casting, Teknik Metalurgi. Universitas Sultan Ageng Tirtayasa (Indonesian Language).
12. Nishimura, T., Tamilselvi, S., Min, X. H., & Tsuzaki, K. Corrosion resistance of aging heat-treated Ti-8Mo-5Fe alloy in highly acidic chloride solution. *Materials Transactions* **2010**; 51(9); pp. 1553–1559.
13. Wang, Z., Huang, W., & Meng, X. Electrochemical behaviour of Ti-25Nb-3Mo-3Zr-2Sn biomedical alloy in different simulated physiological environments. *Materials Science and Technology (United Kingdom)* **2015**; 31(11); pp. 1335–1341.
14. Martins, D. Q., Osório, W. R., Souza, M. E. P., Caram, R., & Garcia, A. Effects of Zr content on microstructure and corrosion resistance of Ti-30Nb-Zr casting alloys for biomedical applications. *Electrochimica Acta* **2008**, 53(6), 2809–2817.
15. ASTM E 1876-01. Dynamic Young's Modulus, Shear Modulus, and Poisson's Ratio by Impulse Excitation of Vibration. *Annual Book of American Society for Testing of Material (ASTM)* **2012**, USA, i, 1–16.
16. Fang, N., Huang, R., Xu, K., Zhang, T., Wu, P., Ma, Y., Cao, H., Qin, J., & Zou, J. Phase Transformation, Microstructures, and Mechanical Properties of $\alpha + \beta$ Two-Phase Titanium Alloy Deposited Metal by Surfacing Welding. *Advances in Materials Science and Engineering* **2022**; 415091; pp. 1-8
17. Yasser Abelrhmn, Gepreel, M. A. H., Kobayashi, S., Okano, S., & Okamoto, T. Biocompatibility of new low-cost (α, + β)-type Ti-Mo-Fe alloys for long-term implantation. *Materials Science and Engineering C* **2019** 99(January); pp. 552–562.
18. Boyer, R., Welsch, G., & Collings, E. W. (1994). Materials properties handbook: titanium alloys.
19. R. Smallman and R. (1999). Bishop, Modern Physical Metallurgy and Materials Engineering.
20. Yumak, N. & Aslantas, K. A review on heat treatment efficiency in metastable btitanium alloys: the role of treatment process and parameters. *JMRT* **2020**; 9(6); pp. 15360-15380.
21. Zhang, Q., Chen, J., Tan, H., Lin, X., & Huang, W. D. (2016). Influence of solution treatment on microstructure evolution of TC21 titanium alloy with near equiaxed β grains fabricated by laser additive manufacture. *J. Alloys Compd.* **2016**; 666; pp. 380–386.
22. Zhu, C., Peng, G., Lin, Y. C., Zhang, X. Y., Liu, C., & Zhou, K. Effects of Mo and Cr contents on microstructures and mechanical properties of near β-Ti alloy. *Materials Science and Engineering A* **2021**; 825(August); p. 141882.
23. Ho, W. F., Wu, S. C., Wang, H. W., & Hsu, H. C. Effects of Cr addition on grindability of cast Ti-10Zr based alloys. *Mater. Chem. Phys.* **2010**; 121(3); pp. 465–471.
24. Giat, S., Nurchamid, J., S, B., Sitompul, & Yuswono. (2012). Pembuatan prototip prostetik sendi lutut. Prosiding InSINas, pp. 1–6 (Indonesian Language).

25. Weiss, I., & Semiatin, S. L. Thermomechanical processing of alpha titanium alloys - An overview. *Mater. Sci. Eng. A.* **1999**; 263(2); 243–256.
26. Zareidoost, A., & Yousefpour, M. A study on the mechanical properties and corrosion behavior of the new as-cast TZNT alloys for biomedical applications. *Mater. Sci. Eng. C.* **2020**; 110(January); p. 110725.
27. Senopati, G.; Rahman Rashid, R.A.; Kartika, I.; Palanisamy, S. Recent Development of Low-Cost β-Ti Alloys for Biomedical Applications: A Review. *Metals* **2023**; 13; p. 194.
28. Senopati, G., Sutowo, C., Kartika, I., & Suharno, B. The Effect of Solution Treatment on Microstructure and Mechanical Properties of Ti-6Mo-6Nb-8Sn Alloy. *Materials Today: Proceedings* **2019**; 13; pp. 224–228.